

Supporting Information

Preparation and characterization of mononuclear complexes $[\text{Fe}(\kappa^2\text{-pdt})(\text{CO})_2(\kappa^2\text{-P}^{\text{Ph}}_2\text{N}^{\text{R}}_2)]$ (R = Ph, Bn)

Scheme S1. Synthesis of complexes $[\text{Fe}(\kappa^2\text{-pdt})(\text{CO})_2(\kappa^2\text{-P}^{\text{Ph}}_2\text{N}^{\text{R}}_2)]$ (R = Ph, Bn).

Figure S1. IR (CH_2Cl_2) (a) and $^{31}\text{P}\{^1\text{H}\}$ NMR (CDCl_3) (b) spectrum of $[\text{Fe}(\kappa^2\text{-pdt})(\text{CO})_2(\kappa^2\text{-P}^{\text{Ph}}_2\text{N}^{\text{Ph}}_2)]$ at 25°C.

Figure S2. IR (CH_2Cl_2) (a) and $^{31}\text{P}\{^1\text{H}\}$ NMR (CDCl_3) (b) spectra of **1** at 25°C.

Figure S3. Comparison of CV of **1-4** under Ar and CO in $\text{CH}_2\text{Cl}_2\text{-}[\text{NBu}_4][\text{PF}_6]$ 0.2 M at $v = 0.2 \text{ V s}^{-1}$.

Table S1. Crystallographic data of $[\text{Fe}_3(\text{CO})_5(\kappa^2\text{-P}^{\text{Ph}}_2\text{N}^{\text{Bn}}_2)(\mu\text{-adt}^{\text{Bn}})(\mu\text{-pdt})]$ (**4**)

Table S2. Crystallographic data of $[\text{Fe}_3(\text{CO})_5(\kappa^2\text{-P}^{\text{Ph}}_2\text{N}^{\text{Ph}}_2)(\mu\text{-pdt})_2]$ (**1**)

Table S3. Selected distances and bond angles for **1**.

Figure S4. IR spectra of **1** in CH_2Cl_2 in the presence of (a) 6 equiv of $\text{CF}_3\text{SO}_3\text{H}$ and (b) after evolution in the IR cell.

Figure S5. $^{31}\text{P}\{^1\text{H}\}$ NMR spectrum of **1** at 243 K in the presence of 3 equiv of $\text{CF}_3\text{SO}_3\text{H}$

Figure S6. ^1H NMR spectrum of **1** at 243 K in the presence of 3 equiv of $\text{CF}_3\text{SO}_3\text{H}$

Figure S7. $^{31}\text{P}\{^1\text{H}\}$ NMR spectrum of **2** at 243 K in the presence of 3 equiv of $\text{CF}_3\text{SO}_3\text{H}$

Figure S8. ^1H NMR spectrum of **2** at 243 K in the presence of 3 equiv of $\text{CF}_3\text{SO}_3\text{H}$

Figure S9. Monitoring in the IR cell of the evolution of $3\text{adt}^{\text{Bn}}\text{H}^+$ in CH_2Cl_2 after 5 min (red curve) and 10 min (purple curve) ; IR spectrum of **3** in CH_2Cl_2 (black curve).

Figure S10. IR (CH_2Cl_2) spectra of complex **4** in the presence of $\text{CF}_3\text{SO}_3\text{H}$: 0 equiv (blue curve), 2 equiv (blue curve) and 6 equiv (purple curve)

Preparation and characterization of mononuclear complexes $[\text{Fe}(\kappa^2\text{-pdt})(\text{CO})_2(\kappa^2\text{-P}^{\text{Ph}}_2\text{N}^{\text{R}}_2)]$ (R = Ph, Bn)

The complexes $[\text{Fe}(\kappa^2\text{-pdt})(\text{CO})_2(\kappa^2\text{-P}^{\text{Ph}}_2\text{N}^{\text{R}}_2)]$ (R = Ph, Bn) were prepared following adaptations of reported procedures ^[42] (Scheme S1). One equivalent of $\text{P}^{\text{Ph}}_2\text{N}^{\text{R}}_2$ (R = Ph (0.644 g, 1.42 mmol), Bn (0.684 g, 1.42 mmol)) was added to a solution of $[\text{FeI}_2(\text{CO})_4]$ (0.60 g, 1.42 mmol) in CH_2Cl_2 . After 2h under vacuum, an IR monitoring showed the complete transformation into the complex $[\text{FeI}_2(\text{CO})_2(\kappa^2\text{-P}^{\text{Ph}}_2\text{N}^{\text{R}}_2)]$. A solution of propanedithiol (0.18 mL, 1.79 mmol) and triethylamine (0.48 mL, 3.58 mmol), in 10 mL of CH_2Cl_2 , were then added to the reaction solution. After 4h of stirring, the solvent was evaporated and the residue was purified by a column chromatography (silica gel) using CH_2Cl_2 :THF (95:5) as eluent. A red band was collected and evaporated to dryness under vacuum which gives red powders of complexes $[\text{Fe}(\kappa^2\text{-pdt})(\text{CO})_2(\kappa^2\text{-P}^{\text{Ph}}_2\text{N}^{\text{R}}_2)]$.

Data for $[\text{Fe}(\kappa^2\text{-pdt})(\text{CO})_2(\kappa^2\text{-P}^{\text{Ph}}_2\text{N}^{\text{Ph}}_2)]$:

m = 0.83 g, yield = 68%

IR (CH_2Cl_2 , cm^{-1}) : $\bar{\nu}(\text{CO}) = 2014$ (s), 1966 (s).

$^{31}\text{P}\{^1\text{H}\}$ NMR (CDCl_3 , ppm) : $\delta = 39.8$ (d, $^2J_{\text{PP}} = 129.5$ Hz), 33.2 (d, $^2J_{\text{PP}} = 129.5$ Hz).

^1H NMR (CDCl_3 , ppm) : $\delta = 7.78 - 7.01$ (m, 20H, Ph), [5.27 (m, 1H), 4.71 (m, 1H), 4.08 (m, 3H), 3.93 (m, 1H), 3.80 (m, 1H), 3.43 (m, 1H)] (4 x CH_2 , $\text{P}^{\text{Ph}}_2\text{N}^{\text{Ph}}_2$), 2.53, 2.47, 2.08 and 1.97 (m, 6H, CH_2 , pdt).

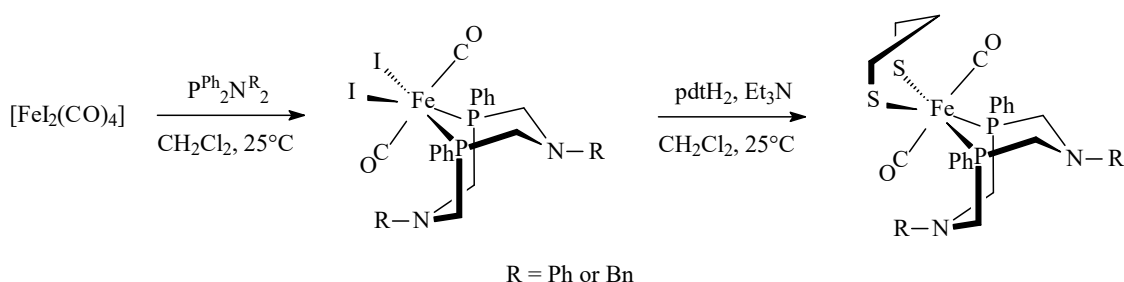
Data for $[\text{Fe}(\kappa^2\text{-pdt})(\text{CO})_2(\kappa^2\text{-P}^{\text{Ph}}_2\text{N}^{\text{Bn}}_2)]$:

m = 0.80 g, yield = 67 %

IR (CH_2Cl_2 , cm^{-1}) : $\bar{\nu}(\text{CO}) = 2012$ (s), 1963 (s).

$^{31}\text{P}\{^1\text{H}\}$ NMR (CDCl_3 , ppm) : $\delta = 38.5$ (d, $^2J_{\text{PP}} = 130$ Hz), 31.7 (d, $^2J_{\text{PP}} = 130$ Hz).

^1H NMR (CDCl_3 , ppm) : $\delta = 7.50 - 7.05$ (m, 20H, Ph), 4.44 (m, 1H, PCH_2N), 4.04 (s, 2H, NCH_2Ph), 3.92 (m, 1H, PCH_2N), 3.69 (m, 2H, NCH_2Ph), 3.28-3.04 (m, 4H, PCH_2N) 3.91 (m, 1H, PCH_2N), 2.60 (m, 1H, PCH_2N) (m, 8H, PCH_2N), 2.48, 2.41, 1.95 and 1.88 (m, 6H, pdt).



Scheme S1. Synthesis of complexes $[\text{Fe}(\kappa^2\text{-pdt})(\text{CO})_2(\kappa^2\text{-P}^{\text{Ph}}_2\text{N}^{\text{R}}_2)]$ (R = Ph, Bn).

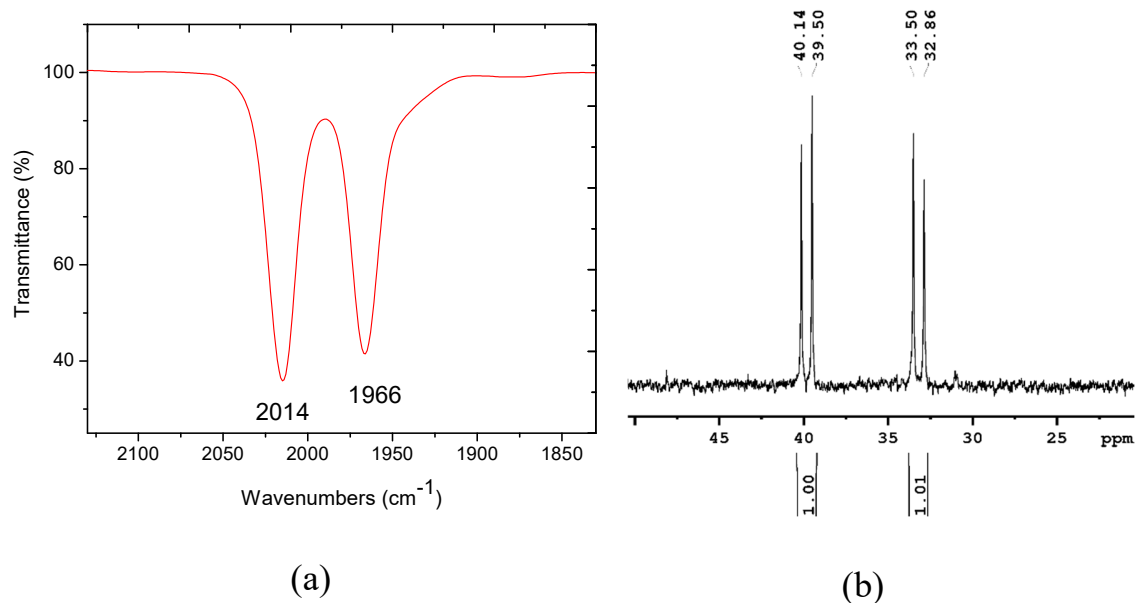


Figure S1. IR (CH_2Cl_2) (a) and $^{31}\text{P}\{^1\text{H}\}$ NMR (CDCl_3) (b) spectrum of $[\text{Fe}(\kappa^2\text{-pdt})(\text{CO})_2(\kappa^2\text{-P}^{\text{Ph}}_2\text{N}^{\text{Ph}}_2)]$ at 25°C.

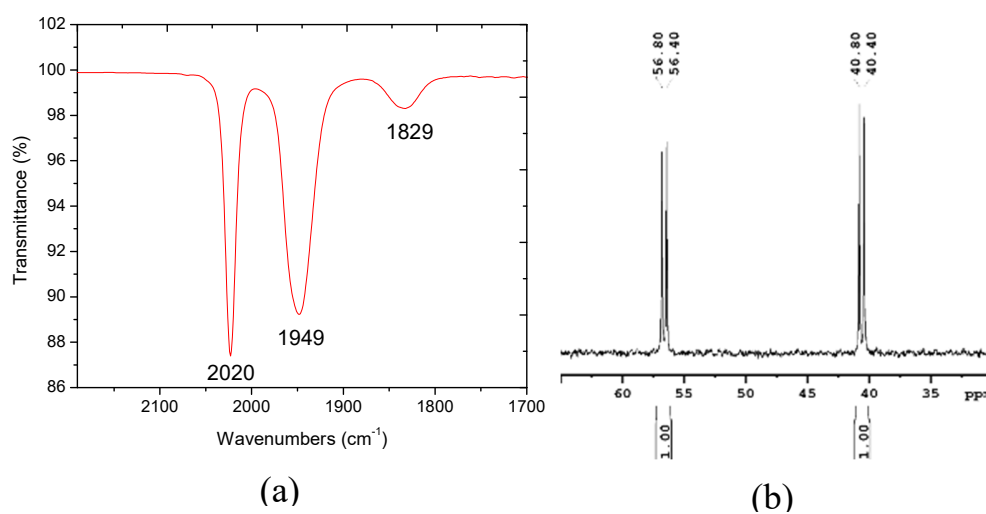


Figure S2. IR (CH_2Cl_2) (a) and $^{31}\text{P}\{^1\text{H}\}$ NMR (CDCl_3) (b) spectra of **1** at 25°C.

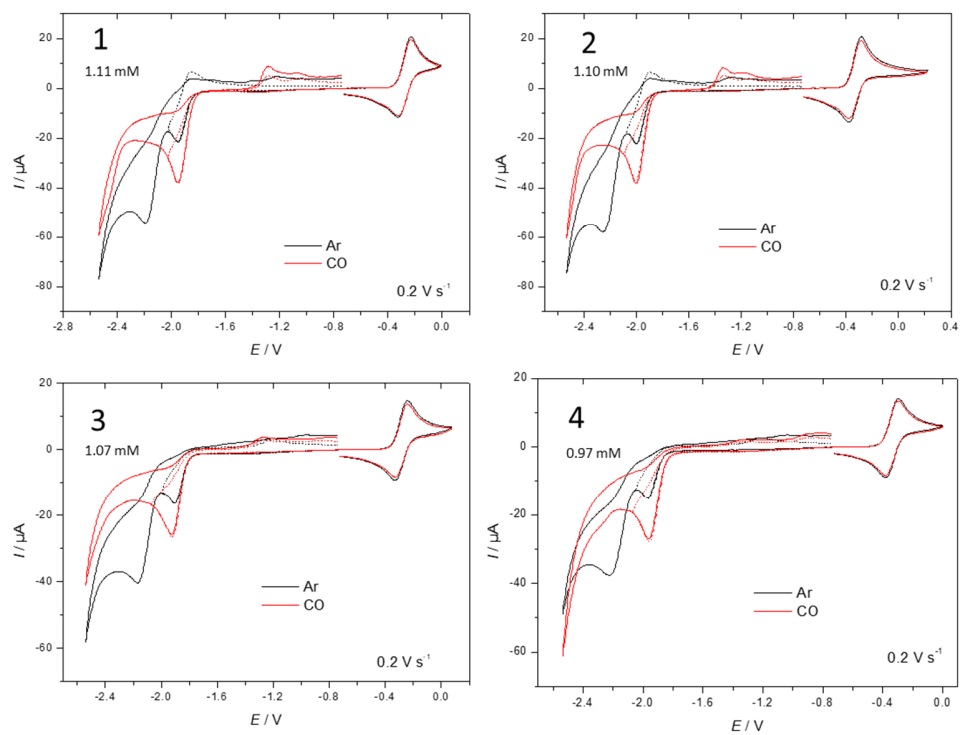


Figure S3. Comparison of CV of **1-4** under Ar and CO in CH_2Cl_2 - $[\text{NBu}_4][\text{PF}_6]$ 0.2 M at $v = 0.2 \text{ V s}^{-1}$.

Table S1. Crystallographic data of $[\text{Fe}_3(\text{CO})_5(\kappa^2\text{-P}^{\text{Ph}}_2\text{N}^{\text{Bn}}_2)(\mu\text{-adt}^{\text{Bn}})(\mu\text{-pdt})]$ (**4**)

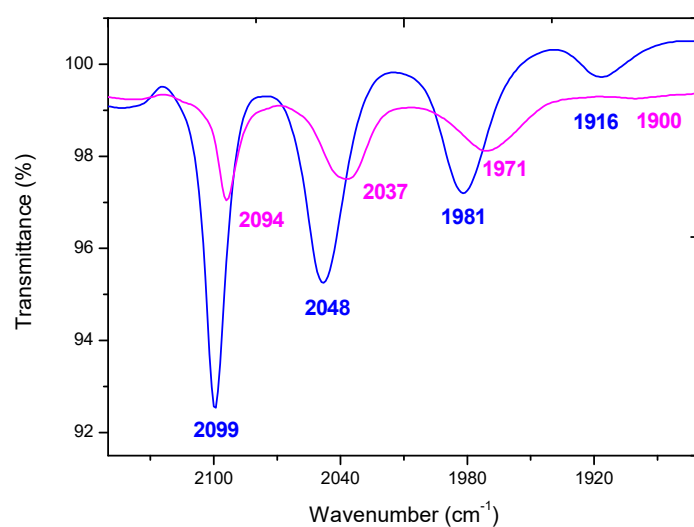
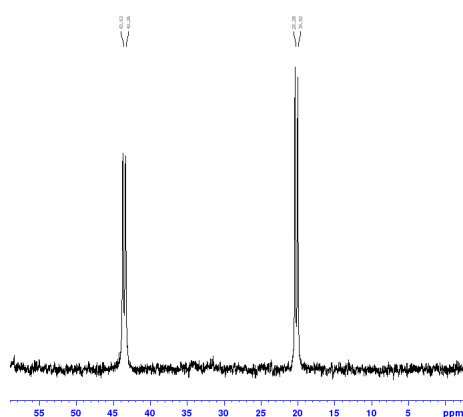
Empirical formula	$\text{C}_{47}\text{H}_{49}\text{Fe}_3\text{N}_3\text{O}_5\text{P}_2\text{S}_4$
Formula weight	1093.62
Temperature/K	150(2)
Wavelength/Å	0.71073
Crystal system	Monoclinic
Space group	P 1 21 1
a (Å)	15.9368(15)
b (Å)	9.1948(6)
c (Å)	17.7390(18)
α (deg)	90
β (deg)	115.510(12)
γ (deg)	90
V (Å ³)	2346.0(4)
Z	2
ρ_{calc} (Mg.mm ⁻³)	1.548
μ (mm ⁻¹)	1.211
$F(000)$	1128
Crystal size (mm)	0.22 x 0.07 x 0.02
Crystal color	Intense red
Crystal shape	Plate // (0 0 1)
Range of ϑ (deg)	3.45 to 26.37
Limiting indices	$-19 \leq h \leq 19, -9 \leq k \leq 11, -22 \leq l \leq 20$
Reflections collected / unique	13114 / 8161
R_{int}	0.0991
Completeness to $\vartheta = 26.37$	99.5
Absorption correction	Analytical
Max. / Min. transmission	0.9762 / 0.7764
Refinement method	Full-matrix least-squares on F^2
Data / Restraints / Parameters	8161 / 1 / 577
R_1 [$I > 2\sigma(I)$]	0.0671
wR_2 [$I > 2\sigma(I)$]	0.0972
R_1 (all data)	0.1186
wR_2 (all data)	0.1283
Goodness-of-fit on F^2	0.969
$\Delta\rho_{\text{max}}, \Delta\rho_{\text{min}}$ /e.Å ⁻³	0.913, -0.717

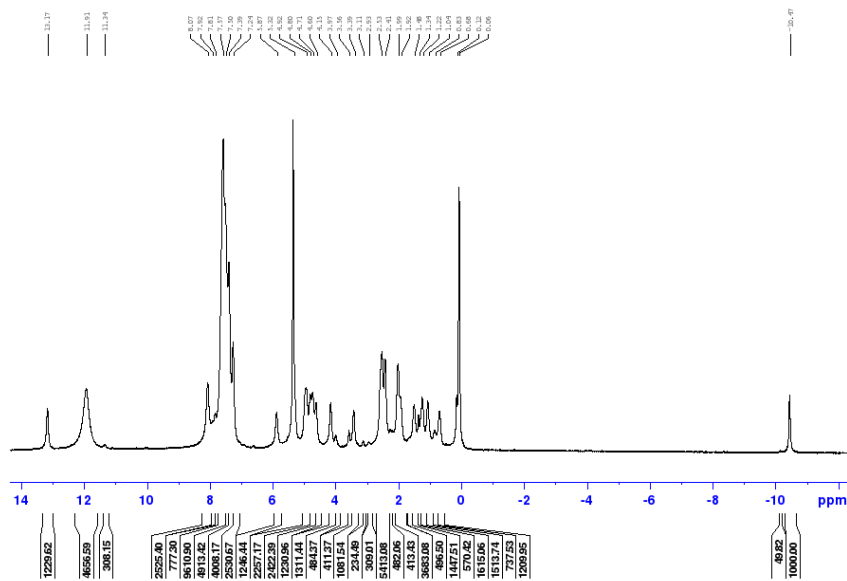
Table S2. Crystallographic data of $[\text{Fe}_3(\text{CO})_5(\kappa^2\text{-Ph}_2\text{NPh}_2)(\mu\text{-pdt})_2]$ (**1**)

Empirical formula	$\text{C}_{39}\text{H}_{40}\text{Fe}_3\text{N}_2\text{O}_5\text{P}_2\text{S}_4$
Formula weight	974.46
Temperature/K	150(2)
Wavelength/Å	0.71073
Crystal system	Orthorhombic
Space group	$Pn\bar{a}21$
a (Å)	17.7651(16)
b (Å)	11.4986(10)
c (Å)	39.489(9)
α (deg)	90
β (deg)	90
γ (deg)	90
V (Å ³)	8067(2)
Z	8
ρ_{calc} (Mg.mm ⁻³)	1.605
μ (mm ⁻¹)	1.398
F(000)	4000
Crystal size (mm)	0.29 x 0.20 x 0.01
Crystal color	Red
Crystal shape	Plate // (0 0 1)
Range of θ (deg)	3.29 to 26.37
Limiting indices	$-22 \leq h \leq 12$, $-14 \leq k \leq 13$, $-49 \leq l \leq 49$
Reflections collected / unique	21073 / 11106
R_{int}	0.1895
Completeness to $\theta = 26.37$	99.7
Absorption correction	Analytical
Max. / Min. transmission	0.9862 / 0.6873
Refinement method	Full-matrix least-squares on F^2
Data / Restraints / Parameters	11106 / 81 / 426
R_1 [$I > 2\sigma(I)$]	0.1599
wR_2 [$I > 2\sigma(I)$]	0.3550
R_1 (all data)	0.2705
wR_2 (all data)	0.4610
Goodness-of-fit on F^2	1.058
$\Delta\rho_{\text{max}}$, $\Delta\rho_{\text{min}}$ /e.Å ⁻³	1.751, -1.860

Table S3. Selected distances and bond angles for **1**.

1			
	<i>Distance (Å)</i>		<i>Angles (°)</i>
Fe1-Fe2	2.531(6)	Fe1-Fe2-Fe3	160.3(3)
Fe2-Fe3	2.556(6)	Fe2-C2-O2	157(3)
Fe1-CO _{terminal}	1.69(3)	Fe1-C2-O2	125(2)
Fe3-CO _{terminal}	1.72(4)-1.86(6)	Fe2-C2-Fe1	77.2(13)
Fe1-CO _{bridging}	2.28(3)	Fe1-Fe2-C2	61.5(11)
Fe2-CO _{bridging}	1.71(3)	P1-Fe1-P2	82.1(4)
Fe1-P1	2.196(11)		
Fe1-P2	2.218(10)		

**Figure S4.** IR spectra of **1** in CH₂Cl₂ in the presence of 6 equiv of CF₃SO₃H (blue curve) and after evolution in the IR cell (purple curve).**Figure S5.** ³¹P{¹H} NMR spectrum of **1** at 243 K in the presence of 3 equiv of CF₃SO₃H



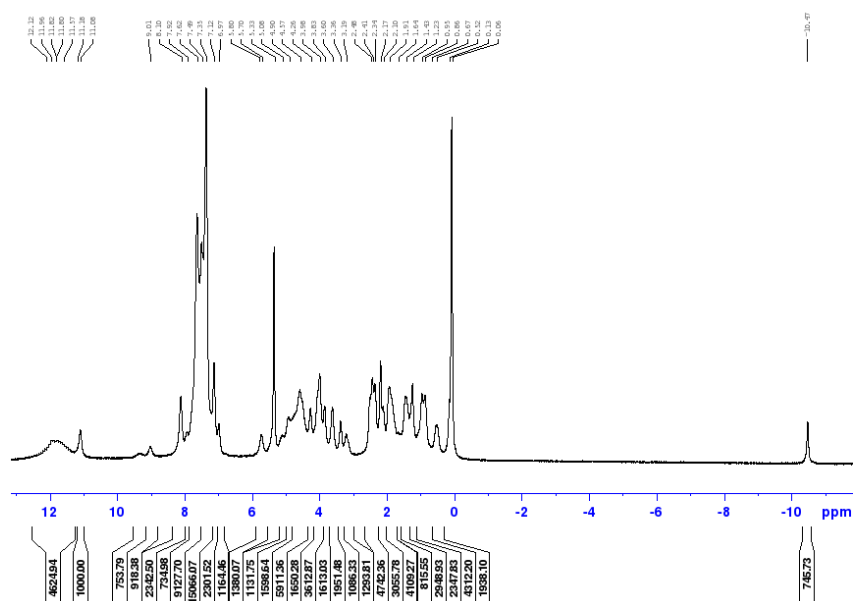


Figure S8. ^1H NMR spectrum of **2** at 243 K in the presence of 3 equiv of $\text{CF}_3\text{SO}_3\text{H}$

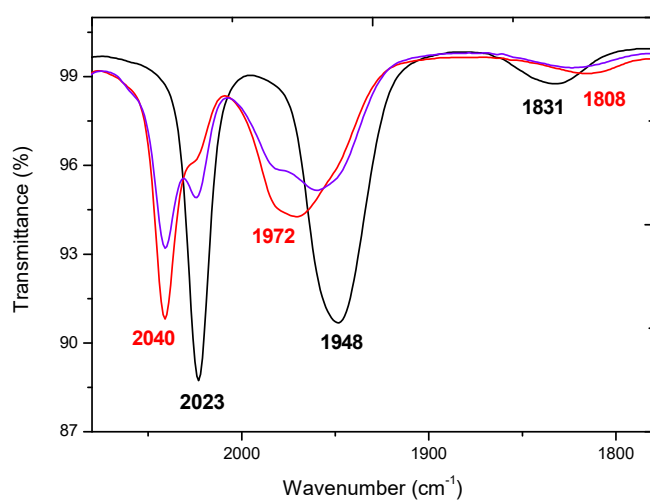


Figure S9. Monitoring in the IR cell of the evolution of $3\text{adt}^{\text{Bn}}\text{H}^+$ in CH_2Cl_2 after 5 min (red curve) and 10 min (purple curve) ; IR spectrum of **3** in CH_2Cl_2 (black curve).

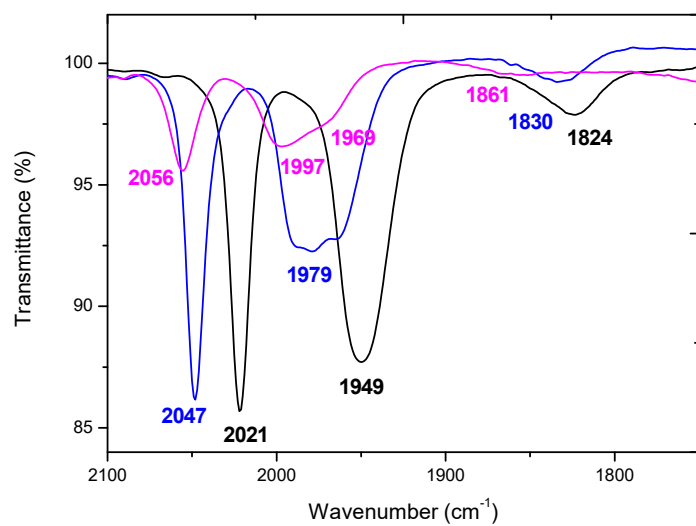


Figure S10. IR (CH₂Cl₂) spectra of complexes **4** in the presence of CF₃SO₃H : 0 equiv (black curve), 2 equiv (blue curve) and 6 equiv (purple curve)